Current Research in Insect Science 6 (2024) 100100

Contents lists available at ScienceDirect

Current Research in Insect Science

journal homepage: www.elsevier.com/locate/cris

α-Glucosidase isoform G contributes to heme detoxification in *Rhodnius prolixus* and its knockdown affects *Trypanosoma cruzi* metacyclogenesis

Fernanda Ferreira Maissner [a], Carina Azevedo Oliveira Silva [c], André Borges Farias [d], Evenilton Pessoa Costa [a], José Luciano Nepomuceno-Silva [c], José Roberto da Silva [b,c], Flávia Borges Mury [a,b,*]

[a] Laboratório Integrado de Biociências Translacionais (LIBT), NUPEM/UFRJ, Macaé, RJ, Brazil
[b] Instituto Nacional de Entomologia Molecular (INCT-EM), Universidade Federal do Rio de Janeiro, Rio de Janeiro, Brazil
[c] Laboratório Integrado de Bioquímica Hatisaburo Masuda (LIBHM), NUPEM/UFRJ, Macaé, RJ, Brazil
[d] Laboratório Integrado de Computação Científica (LICC), CM/UFRJ, Macaé, RJ, Brazil

ARTICLE INFO

Keywords:
American trypanosomiasis
Digestion
Heme
Perimicrovillar membranes
Vector-pathogen interaction

ABSTRACT

The triatomine bug *Rhodnius prolixus* is a hematophagous hemipteran and a primary vector of *Trypanosoma cruzi*, the causative agent of Chagas' disease (CD), in Central America and Northern South America. Blood-feeding poses significant challenges for hematophagous organisms, particularly due to the release of high doses of pro-oxidant free heme during hemoglobin digestion. In this arthropod, most of the free heme in the gut is aggregated into hemozoin (Hz), an inert and non-oxidative biocrystal. Two major components present in the perimicrovillar membranes (PMM) of triatomine insects have been previously implicated in heme crystallization: lipids and the biochemical marker of the PMM, the enzyme α-glucosidase. In this study, we investigated the role of *R. prolixus* α-glucosidase isoform G (Rp-αGluG) in heme detoxification and the effects of its knockdown on the insect physiology. The effect of α-glucosidase isoform G (αGluG) knockdown on *T. cruzi* proliferation and metacyclogenesis was also investigated. Initially, a 3D structure of Rp-αGluG was predicted by comparative modeling and then subjected to molecular docking with the heme molecule, providing *in silico* support for understanding the process of Hz biocrystallization. Next, adult females of *R. prolixus* were challenged with RNAi against Rp-αGluG (dsαGluG) to assess physiological and phenotypic changes caused by its knockdown. Our data show that the group challenged with dsαGluG produced less Hz, resulting in more intact hemoglobin available in the digestive tract. These animals also laid fewer eggs, which had a lower hatching rate. In addition, *T. cruzi* metacyclogenesis was significantly lower in the dsαGluG group. The present work demonstrates the importance of Rp-αGluG in heme detoxification, the digestive and reproductive physiology of *R. prolixus*, as well as its influence on the life cycle of *T. cruzi*. Since heme neutralization is a vital process for hematophagous bugs, our study provides useful information for the development of new strategies targeting the Hz formation and potentially affecting the vectorial transmission of Chagas disease.

1. Introduction

Hematophagy has enabled many arthropod groups to act as vectors in the transmission of a variety of pathogens that cause several diseases of public health importance, such as Chagas Disease (CD) (WHO, 2022), caused by the unicellular eukaryote *Trypanosoma cruzi*. CD is an anthropozoonosis that affects approximately 8 million people worldwide and is endemic to the Americas, but has spread from its original boundaries through migration to 21 countries in Europe, Africa, and occasionally in Asia and Oceania (Patel, 2020; WHO, 2022). Vector borne transmission is limited to both endemic and nonendemic areas of North, Central, and South America (Bern, 2015; Pérez-Molina and Molina, 2018; Mills, 2020). Other infection routes include blood transfusion, organ and bone marrow transplantation, and congenital transmission occur mainly in non-endemic countries (Guarner, 2019; Iglesias-Rus et al., 2019). Food contamination has been predominantly

* Corresponding author at: LIBT-CCS-NUPEM, Universidade Federal do Rio de Janeiro (UFRJ), *Av*. São José do Barreto N° 764 Bairro: São José do Barreto, Macaé, RJ, Brazil.
E-mail address: fbmury@nupem.ufrj.br (F.B. Mury).

https://doi.org/10.1016/j.cris.2024.100100
Received 29 August 2023; Received in revised form 11 October 2024; Accepted 14 October 2024
Available online 16 October 2024

reported in Latin America, where transmission cycles involving wild vector populations and mammalian reservoir hosts are prominent. The infection persists due to the absence of effective early treatment. CD causes approximately 12,000 deaths annually and significantly reduces the life expectancy of the infected population, resulting in negative social impacts (DNDI, 2023). Treatment of the disease is currently limited to the drugs benznidazole and nifurtimox, which are more effective when administered at the initial acute phase of CD. However, the efficacy of these drugs decreases when administered later in the chronic phase of the disease, and the chances of a good prognosis and relief of symptoms are reduced (WHO, 2022). Therefore, other methods of disease control are needed, such as restricting transmission routes, especially transmission by its insect vectors (Pérez-Molina and Molina, 2018).

Rhodnius prolixus (Hemiptera, Reduviidae, Triatominae) is one of the most efficient vectors of *T. cruzi*, the causative agent of CD. It is assumed to have evolved from the ancestral forms of other Rhodniini in or around the Amazon region of South America, becoming highly adapted to domestic and peridomestic habitats - especially in the llanos of Venezuela and Colombia, where it remains a significant domestic vector of *T. cruzi* (Schofield and Galvão, 2009; Justi and Galvão, 2017).

The parasites are taken up from an infected vertebrate blood as trypomastigotes. In the vector midgut, *T. cruzi* develops into epimastigote forms, which are capable of multiplying and colonizing the intestinal tract of hematophagous Triatominae Hemiptera. Later, in the hindgut, under a condition of nutritional restriction, it differentiates into metacyclic trypomastigotes (non-replicative and infective forms) in a process called metacyclogenesis. These trypomastigotes are then excreted in large numbers in insect feces as the triatomines feed on their hosts and can gain immediate access to the bloodstream when dragged to the bite site or mucosal surfaces (Kollien and Schaub, 1999; Ferreira et al., 2016; Melo et al., 2020).

The digestion of blood by hematophagous organisms allows the absorption and utilization of host derived nutrients for their development, survival, and reproduction (Lehane, 2005). In *R. prolixus*, the breakdown of hemoglobin is accomplished by digestive enzymes that lead to the release of heme, which is the prosthetic group of hemoglobin (Terra and Ferreira, 2012; Graça-Souza et al., 2006). Heme, or iron-protoporphyrin IX (Fe(III)PPIX), is a molecule involved in biological processes crucial for the body homeostasis, including oxygen transport (Shimizu et al., 2019). However, free heme is known to cause pro-oxidant effects and induces oxidative stress by the formation of reactive oxygen species (ROS) (Dansa-Petretski et al., 1995; Gutteridge and Smith, 1988; Ryter and Tyrrell, 2000; Stiebler et al., 2011; Shimizu et al., 2019). In addition, since it is a low molecular weight amphiphilic molecule, an overload of heme can lead to several detrimental effects (Ryter and Tyrrell, 2000), such as lipid peroxidation (Schmitt et al., 1993), nucleic acids oxidation (Aft and Mueller, 1983), and cell death (Slimen et al., 2014).

In the gut of *R. prolixus*, most of the free heme is converted into insoluble hemozoin crystals (Hz), which are excreted in the feces (Silva et al., 1995, 2006, 2007; Oliveira et al., 1999). This conversion represents the first line of defense against the oxidative effects of heme in the intestinal lumen (Oliveira et al., 2002; Sterkel et al., 2017). Interestingly, Ferreira et al. (2018) demonstrated that chemical blockage of Hz formation resulted in poorly developed ovaries and fewer eggs laid. In addition, authors showed that *T. cruzi* load was strongly reduced under such conditions.

In addition to Hz formation, other compensatory defense mechanisms such as antioxidant enzymes, the hemoxisomes, urate, and the hemolymphatic *Rhodnius* Heme-Binding Protein (RHBP), also help to combat heme overload and its oxidative effects (Dansa-Petretski et al., 1995; Souza et al., 1997; Paes and Oliveira, 1999; Paes et al., 2001; Braz et al., 2002; Silva et al., 2006; Ferreira et al., 2018).

Silva et al. (2007) reported the involvement of gut lipid and protein components in heme crystallization in *R. prolixus*. The lipid fraction is a major component of the perimicrovillar membranes (PMM) present in the gut of Hemiptera, and the protein fraction associated with the PMM contains considerable amounts of the enzyme α-glucosidase (Silva et al., 2007). In most species, this enzyme is involved in the primary metabolism of oligosaccharides. In this arthropod, however, it plays a crucial role in the Hz formation (Mury et al., 2009). According to the proposed model of Hz formation, this enzyme is involved in the nucleation step by assisting in the clustering of heme molecules, at the beginning of the process (Stiebler et al., 2011). Genome sequencing of *R. prolixus* revealed that there are seven α-glucosidase isoforms encoding genes, whose products are either membrane-associated or soluble (Ribeiro et al., 2014; Mesquita et al., 2015).

Once unveiling which α-glucosidases are involved in the heme detoxification process, it may reveal new molecular targets for novel drugs to control CD and its vector, *R. prolixus*. In the present work, we have investigated the role of Rp-αGluG in a heme detoxification route and in the biology of this triatominae. We also present evidence that its knockdown has an impact on *T. cruzi* metacyclogenesis.

2. Materials and methods

2.1. Bioinformatic analyses

The phylogenetic analysis utilized 32 sequences of the hemipteran alpha-glucosidase enzyme (Supplementary Table S1) and MEGA XI software (Tamura et al., 2021). The protein sequences were aligned using the Muscle tool, and a phylogenetic tree was estimated using the maximum likelihood method. To root the phylogenetic tree, the *Drosophila virilis* sequence (B4LLB7) was used as an outgroup. The phylogeny test was conducted using the bootstrap method with 500 replications. The resulting phylogenetic tree illustrates the hypothetical evolutionary relationships between protein sequences.

The alpha-glucosidase sequence, identified by the VectorBase database (https://vectorbase.org/vectorbase/app/record/gene/RPRC013046) with the ID RPRC013046, was subjected to a Blast search against the PDB database on the NCBI server. This search aimed to identify proteins with similar sequences that could serve as templates for constructing a three-dimensional model of alpha-glucosidase via comparative modeling. As a result, the PDB template with the ID 6LGA with 1.85 Å of resolution (Miyazaki and Park, 2020) was identified, exhibiting a coverage and identity of 95% and 39%, respectively. A homology based three-dimensional structure of Rp-αGluG was predicted using the Swiss-Model server (Waterhouse et al., 2018). The initial model was submitted to energy refinement in the ModRefiner (Xu and Zhang, 2011). The geometric parameters of structures were validated with PROCHECK (Laskowski et al., 1993) from the UCLA-DOE LAB (saves.mbi.ucla.edu) server, which generated the Ramachandran plot (Table S1). Molecular docking was performed with the software GOLD v.5.8.1 (Jones et al., 1997). The parameters for docking were determined by analysis of poses obtained by redocking of a homologous protein (PDB ID 6LGB; Miyazaki and Park, 2020) co-crystallized with alpha-d-glucopyranose. The comparison between the co-crystallized structure and the preferred conformation obtained by redocking revealed an RMSD value of 0.39 Å, indicating the satisfactory quality of the parameters for the molecular docking study. Therefore, the docking was performed with Goldscore function with a 10 Å of distance from His352 (NE2 id 5398). ChemAxon program (http://www.chemaxon.com) was used to build and protonate the heme molecule, considering pH 5.4, which was subsequently minimized using the PM3 method in the Gaussian 03 W program (Frisch, 2004). The visual inspection of intermolecular interactions and figures were generated using PyMOL v.2.4.0a0 (Schrödinger, 2015).

2.2. Ethics statement

All animal care and experimental protocols were conducted in accordance with the guidelines of the Committee for Evaluation of

Animal Use for Research (Federal University of Rio de Janeiro – NUPEM/CCS) and the protocols were approved by CCS-UFRJ, under register 01,200.001568/2013–87.

2.3. Insects

A colony of *R. prolixus* was kept in an incubator (FT 1020 model – DeLeo) at 28 °C and 70–80% relative humidity, at the Institute of Biodiversity and Sustainability – NUPEM – UFRJ and fed onto the ear of live rabbits every 28 days. This colony was first started with insects derived from a colony at Leopoldo de Meis Institute for the Biochemistry of Medicine – UFRJ. The adult females challenged with dsRNA of Rp-αGluG and dsGFP were fed in two different ways: females were fed directly into the rabbit ear for standard experiments or alternatively females were fed in an artificial feeder at 37 °C, in case of *T. cruzi* infection, detailed below. The post-feeding intervals were determined by the specific conditions of each experiment. The details of the post-feeding duration for each experiment are provided in the subsequent sections.

2.4. dsRNA synthesis

The DNA template for dsRNA synthesis was made up using cDNA from *R. prolixus*' posterior midgut. dsRNA from GFP (dsGFP) was used as control and synthetized from a Green Fluorescent Protein (EGFP) gene cloned on a pGEM®-T Easy vector (Promega) (Gama et al., 2022). Both dsαGluG and the control dsGFP were synthesized and used in the bioassays. The PCR reactions were performed using GoTaq® Flexi DNA Polymerase Kit (Promega – Cat. No. M8295), followed by purification of products with Wizard® SV Gel and PCR Clean-Up System Kit (Promega – Cat. No. A9282) and quantification on NanoDrop™ (Thermo Scientific). Then, the dsRNA was synthetized using T7 RiboMAX™ Express RNAi System Kit (Promega – Cat. No. P1700) from 1 μg of template DNA. On each step, a 1% agarose gel stained with ethidium bromide was used to confirm the template integrity. Nucleotides in bold lowercase letters in the primers were used in a second PCR reaction to add T7 promoter sites at the ends. All primers for dsRNA synthesis contained the T7 sequence adaptor on their 5′ ends, which is recognized by T7 RNA polymerase (Table S2).

2.5. RNA interference-mediated knockdown of α-glucosidase

The dsRNA solutions (4 μg 2 μL^{-1}) were injected into the thoracic hemolymph of adult females using a Hamilton syringe (Paim et al., 2013a) with a needle outer diameter of 0.05 mm, which avoided mortality and considerable damage to the insect cuticle. The injected insects were fed with rabbit blood on the following day. Four days after blood feeding, posterior midguts were dissected and homogenized in 500 μL TRIzol™ (ThemoFisher – Cat. No. 15,596,026), and total RNA was extracted according to the manufacturer's protocol. Then, the RNA was quantified on NanoDrop™ and 2 μg were used to synthetize cDNA, with High Capacity cDNA Reverse Transcription Kit (Applied Biosystems™ – Cat. No. 4,368,814).

The qPCR was performed using qPCRBIO SyGreen Mix Hi-ROX Kit (PCR Biosystems – Cat. No. PB20.12–05) and reaction carried out on QuantStudio 3 (Applied Biosystems) using Rp-αGluG primers, and Rp-EF-1 (*Rhodnius prolixus Elongation Factor 1*) as endogenous control (VectorBase Gene ID: RPRC015041; Majerowicz et al., 2011) (Table S2).

2.6. Alpha-glucosidase activity

Alpha-glucosidase activity assays were performed with midgut protein extracts to confirm the success of Rp-αGluG knockdown. Midgut epithelium samples from rabbit blood fed *R. prolixus* were obtained 4 days after feeding, homogenized in 1 mL of phosphate-buffered saline 0.1 M pH 7.4, centrifuged for 30 min at 15,000 g at 4 °C and the supernatants were discarded. This procedure was repeated three times, and the resulting pellets were resuspended in 400 μL of extraction buffer (sodium phosphate 20 mM pH 7.4, Triton X-100 0.1%, imidazole 5 mM, PMSF 1 mM and benzamidine 1 mM) and incubated overnight at 4 °C. After that, the sample was centrifuged for 30 min at 15,000 g at 4 °C and the supernatant was used as source of enzyme. Alpha-Glucosidase activity was determined using p-nitrophenyl α-d-glucopyranoside (10 mM) (Sigma Ltd.) in 100 mM citrate phosphate buffer (pH 5.5) as substrate and by following the appearance of p-nitrophenolate, according to the method described by Terra et al. (1988). All assays were performed at 30 °C. Incubations were carried out for at least four different periods of time (15, 30, 45 and 60 min). Reactions were stopped with 200 μL of Na_2CO_3 0.5 M and initial rates of hydrolysis were calculated. The absorbance of released p-nitrophenolate was read in a GBC-UV/Vis-920 spectrophotometer (Multiskan GO – ThermoFisher) at 410 nm. One unit of enzyme was defined as the amount required to hydrolyze 1 μmol of substrate per minute in the assay conditions.

2.7. Hemozoin extraction

Hz was extracted from the midgut of *R. prolixus* as previously described (Oliveira et al., 1999). The midgut contents of 2 blood-fed *R. prolixus* were collected in cold 100 μL phosphate-buffered saline 0.1 M pH 7.4, four days after feeding. Tissues were used for qPCR analysis and the suspensions were centrifuged at 20,000 g for 15 min. The insoluble pigment was further purified by washing three times with $NaHCO_3$ 0.5 M, SDS 2.5%, pH 9.2 and twice with deionized water. The final sediments were solubilized in NaOH 0.1 N and samples containing purified Hz were quantified in a MultiSkan Go spectrophotometer (Thermo Scientific) at 400 nm.

2.8. Hemoglobin content

To analyze whether there was any impairment in blood digestion, foreguts were dissected, homogenized in 50 μL of phosphate-buffered saline 0.1 M pH 7.4 and centrifuged at 14,000 g for 15 min at 4 °C. The supernatant was added to native sample buffer (Tris–HCl pH 6.8 100 mM, glycerol 20%, bromophenol blue 0.02%). For this experiment, samples were submitted to a native PAGE (6% stacking and 12% running gel) run at 20 mA. The gels were fixed in 12.5% trichloroacetic acid for 30 min, followed by a wash with deionized water for the same period. Finally, the gels were revealed in a solution containing 20 mg of dimethoxybenzidine (DMB) solubilized in 18 mL of deionized water, 2 mL of sodium citrate buffer 0.5 M pH 4.5 and 40 μL of 30% H_2O_2. Densitometric analyses were performed with ImageJ (v. 1.46), considering the control group (dsGFP) as a normalizer.

2.9. H_2O_2 formation

Oxidant levels in the posterior midgut were evaluated to assess the redox status of the microenvironment. For this purpose, Amplex™ Red Kit (Thermo Fisher Scientific – Cat. No. A22188) was used for detection of hydrogen peroxide (H_2O_2) and/or peroxidase activity. The epithelium midguts were dissected four days after feeding, homogenized in 100 μL phosphate-buffered saline 0.1 M pH 7.4 and centrifuged at 12,000 g for 15 min at 4 °C. The supernatants were incubated with the reaction mixture and the products of reactions were quantified by spectrophotometry at 560 nm. For evaluation by fluorescence microscopy detection, individual dissected epithelium samples were incubated in the same reaction mixtures for 20 min and visualized on a stereo microscope model M205FA (Leica), containing a DSR ET fluorescence filter.

2.10. Oviposition, hatching and survival

For each experiment, five females were separated from both control and knockdown groups and the laid eggs were collected every 4 days,

until reaching 28 days after feeding. The hatching and mortality rates were monitored for 40 days after blood feeding. The overall morphology of the eggs was also evaluated by observation with a stereo microscope.

2.11. *T. cruzi* infection

Epimastigotes from Dm28c *T. cruzi* lineage were cultivated in LIT medium supplemented with 10% fetal bovine serum, 10,000 U/L penicillin, 10 mg/L streptomycin and 0.0025% hemin at 28 °C. For infection experiments, the blood was collected from marginal veins of a rabbit, with a heparinized syringe, and then centrifuged at 3000 g for 10 min at 24 °C. The plasma was incubated at 56 °C for 2 h to inactivate the complement system. Red blood cells were washed 3 times with phosphate-buffered saline 0.1 M pH 7.4, centrifuged under the same conditions described above, and resuspended in the inactivated plasma. *R. prolixus* females were fed artificially with blood containing 10^7 epimastigotes/mL, as described by Azambuja and Garcia (1997) and Guarneri (2020). The parasite load in the hindgut lumen was evaluated at 7, 14 and 21 days after infection. Infected insects were dissected, and hindgut samples were homogenised in 100 μL of phosphate-buffered saline 0.1 M pH 7.4. The number of parasites was determined by counting in a Neubauer chamber. *T. cruzi* epimastigotes were differentiated from metacyclic trypomastigotes based on their characteristic morphologies and motility patterns. Intermediate stages were considered as epimastigotes.

2.12. Statistical analysis

Data from all quantitative experiments were submitted to a Shapiro-Wilk normality test. For most experiments, statistical comparison was performed using the parametric Student's *t*-test with unpaired data. For the RT-qPCR data were compared with non-parametric Mann-Whitney test. Differences were considered significant whenever $p \leq 0.05$. All statistical analysis were performed using GraphPad Prism 8 (v 8.0.1; GraphPad Software, San Diego, California USA).

3. Results

3.1. Evolutionary analysis of α-glucosidase isoform G from *R. prolixus*

In this study, we conducted a comparative analysis of 32 deduced amino acid sequences of α-glucosidase isoforms derived from various species, including *R. prolixus* (RPRC006247, RPRC010194, RPRC012963, RPRC006918, RPRC012570, ACI96031, RPRC013046, RPRC007096), *Cimex lectularius* (A0A8I6RGT7, A0A8I6RXP7, A0A8I6RXS2, A0A8I6S7S3, A0A8I6S9G1), *Panstrongylus lignarius* (A0A224XA41, A0A224×6Q8, A0A224XGR4, A0A224XH82, A0A224XHG6, A0A224XIW2, A0A224XJG5), *P. megistus* (A0A069DVS1, A0A069DX91), *Pristhesancus plagipennis* (A0A2K8JSD1, A0A2K8JWU1), *R. neglectus* (A0A0P4VHZ7, A0A0P4VP68, A0A0P4VMN3, A0A0P4VMU2), *Triatoma dimidiata* (A0A0V0G4S7), *T. infestans* (A0A023EYE6, A0A16 1N196), and *D. virilis* (B4LLB7). The latter served as an outgroup for the analysis (Fig. 1A).

Our phylogenetic analysis, inferred by Maximum Likelihood, revealed that the F isoform of *R. prolixus* is the most basal among the Hemiptera isoforms, with the node that unites the F isoform and the others presenting a 60% bootstrap support. This position of the F isoform in the topology of the tree was expected, since, after the publication of the *R. prolixus* genome by Mesquita et al. (2015), we were unable to find the sequence of the F isoform in the genome databases. Furthermore, when we compared the sequence of the F isoform with the GenBank database, using the BLAST tool we found greater similarity of the F isoform (Mury et al., 2009) with species of the order Diptera. Except for the F isoform, the G isoform of *R. prolixus* is the most basal among all

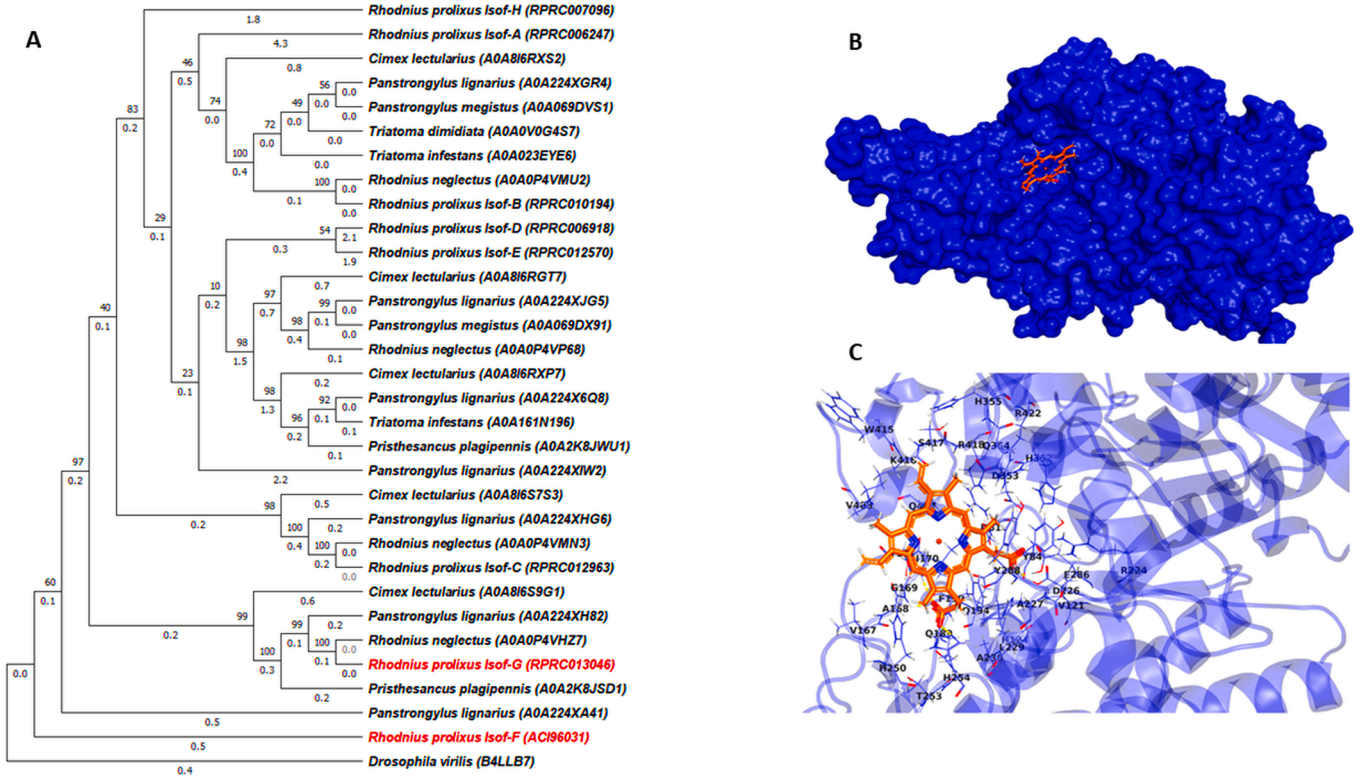

Fig. 1. *In silico* analysis of Rp-αGluG. (A) The phylogenetic tree shows alpha-glucosidase sequences from eight Hemiptera species. The tree was constructed using the maximum likelihood method and a phylogenetic test with bootstrap by 500 replications on MEGA XI software (Tamura et al., 2021). The outgroup used was *Drosophila virilis* (B4LLB7). (B) Molecular docking between Rp-αGluG and heme molecule, showing the cavity that fits this ligand and contains histidine and aspartic acid residues. (C) The cavity marked in C, with all the aminoacids that heme can possibly interact with in a space of 5 Å.

isoforms documented for *R. prolixus* and is therefore the most similar to that published by Mury et al. 2009. Isoform A of *R. prolixus* is most similar to isoform B, both known to be soluble and have no role in heme detoxification (Supplementary Fig. S1).

To evaluate whether Rp-αGluG can be directed to the exocytic pathway for secretion by cells or inserted into the plasma membrane, we conducted a signal peptide analysis using SignalP 6.0 server. Our results indicate an endoplasmic reticulum targeting peptide at the N-terminus, specifically in the first 21 amino acids (Supplementary Fig. S2). Also, we performed a dimensional representation of PRED-TMBB prediction, indicating the corresponding aminoacids on the transmembrane region as well as the prediction of the loops in the outer portion of the membrane (Supplementary Fig. S2).

We also constructed a 3D homology-based model of Rp-αGluG and used molecular docking with heme (Fig. 1B, Supplementary Fig. S3). It is noteworthy that heme can bind to a protein cavity that exposes histidine and aspartic acid residues. Mury et al. (2009) proposed that these residues play a fundamental role in heme binding and Hz formation. Fig. 1C shows the amplified version of Fig. 1B and depicts the potential amino acids that may bind heme. Previously, we determined the potential docking site of heme molecule, with evident contribution of both aminoacids residues (Supplementary Fig. S3).

3.2. Knockdown of *R. prolixus* α-glucosidase isoform G significantly reduces Hz formation

We examined the dynamic of blood digestion post feeding. The average volume ingested per female after blood feeding (Supplementary Fig. S4) and total protein levels measured in the anterior midgut (AM), in the Rp-dsαGluG group and the control, were equivalent at four days after feeding (Supplementary Fig. S5), indicating that blood digestion was progressing normally in both groups. Thus, the investigation of Rp-αGluG role in heme biocrystallization involving gene knockdown in *R. prolixus* (dsαGluG), highlighted the significant decrease on the parameters of RT-qPCR (Fig. 2A), enzymatic activity assessment of α-glucosidase (Fig. 2B) and Hz formation (Fig. 2C), four days after feeding, confirming the effectiveness of Rp-αGluG knockdown and its physiological effects. Analyzing another isoform for comparison, we performed the knockdown of the Rp-αGluA gene that indicated no effect on hemozoin formation, suggesting that this isoform is not involved in the process (Supplementary Fig. S6). Therefore, our results of *in silico* analysis of Rp-αGluG indicate important features of a PMM biomarker, and *in vivo* experiments demonstrated that dsαGluG reduced both enzyme expression and activity, resulting in reduced efficiency of Hz production, confirming the involvement of Rp-αGluG in the process of heme biocrystallization.

3.3. Knockdown of α-glucosidase isoform G delays hemoglobin digestion

When preparing the samples for Hz quantification, we noticed that the supernatant from the midguts of females injected with dsαGluG was reddish (data not shown), that was not seen in the control samples. This could be an indication of a heme fraction not converted into Hz and/or the presence of hemoglobin not fully digested. We performed a quantification of total protein, but there was no significant difference (Supplementary Fig. S5). Thus, we quantified the hemoglobin content by native polyacrylamide gel through band densitometry, four days after feeding. Females injected with dsαGluG showed higher levels of available hemoglobin if compared to control (Fig. 3A).

Since dsαGluG caused a reduction in the content of Hz, we evaluated whether lower expression of Rp-αGluG would also be associated with redox imbalance in the midgut. To this end, we quantified H_2O_2 formation in the midgut, four days after blood feeding. The levels of midguts H_2O_2 trend to be higher in the dsαGluG group when compared to dsGFP (Fig. 3B). When analyzing the midguts under a fluorescence stereo microscope, midgut of females injected with dsαGluG were positively stained for H_2O_2, both on the margins of the posterior midgut epithelium as well as in its inner side, suggesting a more oxidative environment than the control group (Fig. 3C). Our results show that dsαGluG affects heme biocrystallization and delays hemoglobin digestion, which is associated with higher levels of ROS and a more oxidative environment.

3.4. RNAi sensitivity leads to important physiological effects in dsαGluG injected insects

In addition to the digestive process, there are several other processes that are triggered by blood feeding. For example, the process of ecdysis, in the case of nymphs, and the process of oogenesis, in the case of adult females (Buxton, 1930; Atella et al., 2005; Pascual et al., 2021). Oviposition was observed every four days until reaching a period of 28 days after feeding. Egg hatching rate and nymph survival were analyzed for 40 days after both dsαGluG injection and unrelated dsGFP.

In both groups (dsGFP and dsαGluG), there was no difference in the survival rate of females, which was 100%, nor in the total number of eggs (data not shown). However, the spatio-temporal distribution on the number of eggs on each specific day (Fig. 4A) for dsαGluG females showed a significant reduction four and eight days after feeding, when compared to the dsGFP group.

Regarding the hatching process, at the end of a period of 40 days after blood feeding and 20 days after the first record of nymph hatching, we observed that the number of nymphs in dsαGluG group was significantly reduced, if compared to dsGFP (Fig. 4B). In addition, the number

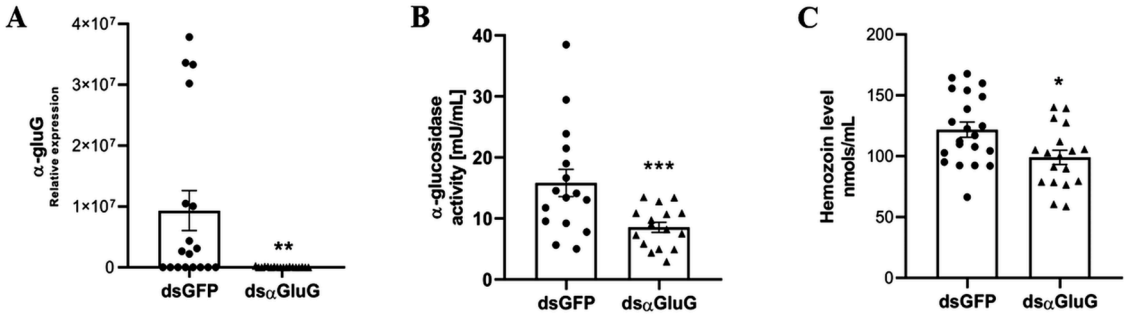

Fig. 2. Knockdown of α-glucosidase isoform G significantly reduces Hz formation. (A) RT-qPCR of posterior midgut, four days after feeding, with significantly reduced relative expression of Rp-αGluG. Statistical analysis using Mann-Whitney test, of three independent experiments. (dsGFP – $n = 18$; dsαGluG – $n = 18$; ** $p = 0.0014$). (B) α-glucosidase activity in the posterior midgut, four days after feeding. Compared to the control group (dsGFP), a significant reduction upon treatment with dsαGluG. (dsGFP – $n = 4$; dsαGluG – $n = 4$; *** $p = 0.0006$) was observed. Mean and SEM of two independent experiments with paired Student's *t*-test. Enzyme activities were carried out at 4 different periods of 15-minutes. (C) Hz formation four days after feeding. Compared to the injected control group (dsGFP), a significant difference was observed, using unpaired Student's *t*-test, expressed with mean and SEM. (dsGFP – $n = 21$; dsαGluG – $n = 18$; * $p = 0.0121$). dsGFP: control females injected with dsRNA unrelated GFP; dsαGluG: females injected with Rp-αGluG).

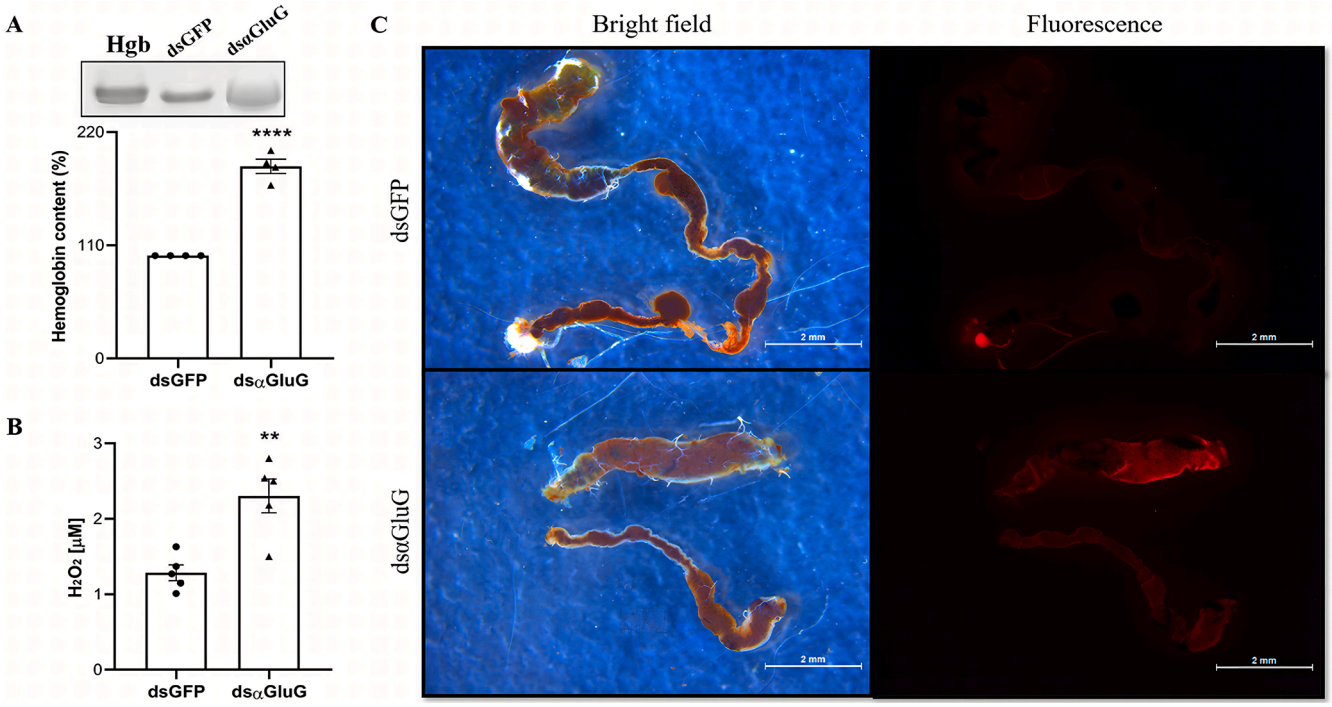

Fig. 3. Knockdown of α-glucosidase isoform G increases remaining hemoglobin and H_2O_2 levels. (A) Females' foregut from insects injected with dsαGluG show higher residual hemoglobin levels if compared to females injected with dsGFP (controls). Hgb: Hemoglobin; dsGFP, females injected with unrelated double strand RNA; dsαGluG, females injected with dsRNA of Rp-αGluG. (dsGFP - $n = 4$; dsαGluG - $n = 4$; **** $p < 0.0001$). (B) Quantification of H_2O_2 content in the posterior midgut, showing significant higher levels of ROS in females injected with dsαGluG, if compared to control. dsGFP: females injected with unrelated double strand RNA; dsαGluG: females injected with Rp-αGluG. (dsGFP – $n = 5$; dsαGluG – $n = 6$; * $p = 0.0034$). Statistical analysis using unpaired *t*-test and expressed with mean and SEM (A, B). (C) Tissue analysis shows fluorescence staining in the posterior midgut in females injected with dsαGluG compared to control. Amplex Red Fluorescence images on the right are correspondent to the brightfield on the left. Scale bar=2mm. (dsGFP – $n = 2$; dsαGluG – $n = 2$).

of eggs per female in dsαGluG group was smaller if compared to the control (dsGFP) (Fig. 4C). As for the remaining eggs, the morphology in dsαGluG group presents an uneven distribution of the contents inside, also showing a proportion of deformations higher when compared to the control (Fig. 4D).

3.5. *Knockdown of α-glucosidase isoform G impacts T. cruzi metacyclogenesis in the hindgut*

Since the Rp-αGluG isoform plays a role in heme detoxification, we checked whether its knockdown would affect *T. cruzi* proliferation and metacyclogenesis. To quantify the parasite load, rectums were collected and conditioned individually, 7, 14 and 21 days after *T. cruzi* infection. We recorded the numbers of the different evolutive forms, namely epimastigotes (replicative form) and metacyclic trypomastigotes (infective form). We also performed RT-qPCR during the three timepoints of infection, and a significant reduction on mRNA of Rp-GluG was observed, showing that the RNAi effect endures, at least, the entire period of the infection (Supplementary Fig. S7). We observed that females injected with dsαGluG presented an apparent increase in the number of epimastigotes at 7 days after infection. At 14 and 21 days, parasite numbers in hindgut of both dsαGluG and dsGFP hindgut were apparently equal (Fig. 5A). On the other hand, trypomastigotes parasite load (Fig. 5B) indicates a similar profile between the dsαGluG and dsGFP groups, 7 and 14 days after infection, but on the 21st day of infection, there was a more noticeable difference, suggesting fewer trypomastigote form in the rectum of females injected with dsαGluG. We calculated the metacyclogenesis rate based on the ratio of the metacyclic trypomastigotes over the total number of parasites found in the hindgut, which depicted the difference (Fig. 5C). In addition, hemozoin formation was also measured 7, 14 and 21 days after infection, but no significant difference was observed between groups (data not shown).

Our results suggest that the physiological environment induced by dsαGluG seemed to favor epimastigote proliferation at the 7 initial days post infection, but this difference was not sustained later days upon infection. However, knockdown of αGluG is detrimental to metacyclogenesis, thereby impairing the emergence of infectious forms critical for pathogen transmission.

4. Discussion

The heme molecule is involved in biological processes such as oxygen transport and signal transduction, however, in its free form it promotes oxidative stress by generating ROS (Gutteridge and Smith, 1988; Dansa-Petretski et al., 1995; Ryter and Tyrrell, 2000; Stiebler et al., 2011; Shimizu et al., 2019), such as superoxide anion (O^2-), hydrogen peroxide (H_2O_2) and hydroxyl radical (OH) (Mittler, 2002). During blood digestion in the midgut of *R. prolixus*, huge amounts of heme are released, posing an important oxidative threat to the bug. The main line of defense against the toxic effects of hemoglobin digestion is the formation of Hz, an inactive and insoluble crystal of heme (Silva et al., 1995; Oliveira et al., 1999; Graça-Souza et al., 2006; Silva et al. 2007) that is synthesized in the PMMs (Silva et al., 2004, 2007). Hz formation, in addition to other strategies to overcome heme toxicity (Graça-Souza et al. 2006), is a very efficient mechanism for reducing heme availability and redox imbalance in the gut of hematophagous organisms such as *R. prolixus* (Oliveira et al., 2000; Mury et al., 2009; Ferreira et al., 2018). Previous works have revealed the significance of Hz formation in heme detoxification and upkeep of redox balance in *R. prolixus* midgut (Oliveira et al., 2000; Mury et al., 2009; Ferreira et al., 2018).

Even though the importance of Hz formation to biological systems is well recognized, the mechanism of its formation is still not fully understood. Earlier studies suggested the involvement of a so-called heme polymerase, and a few proteins have been considered for this role (Slater

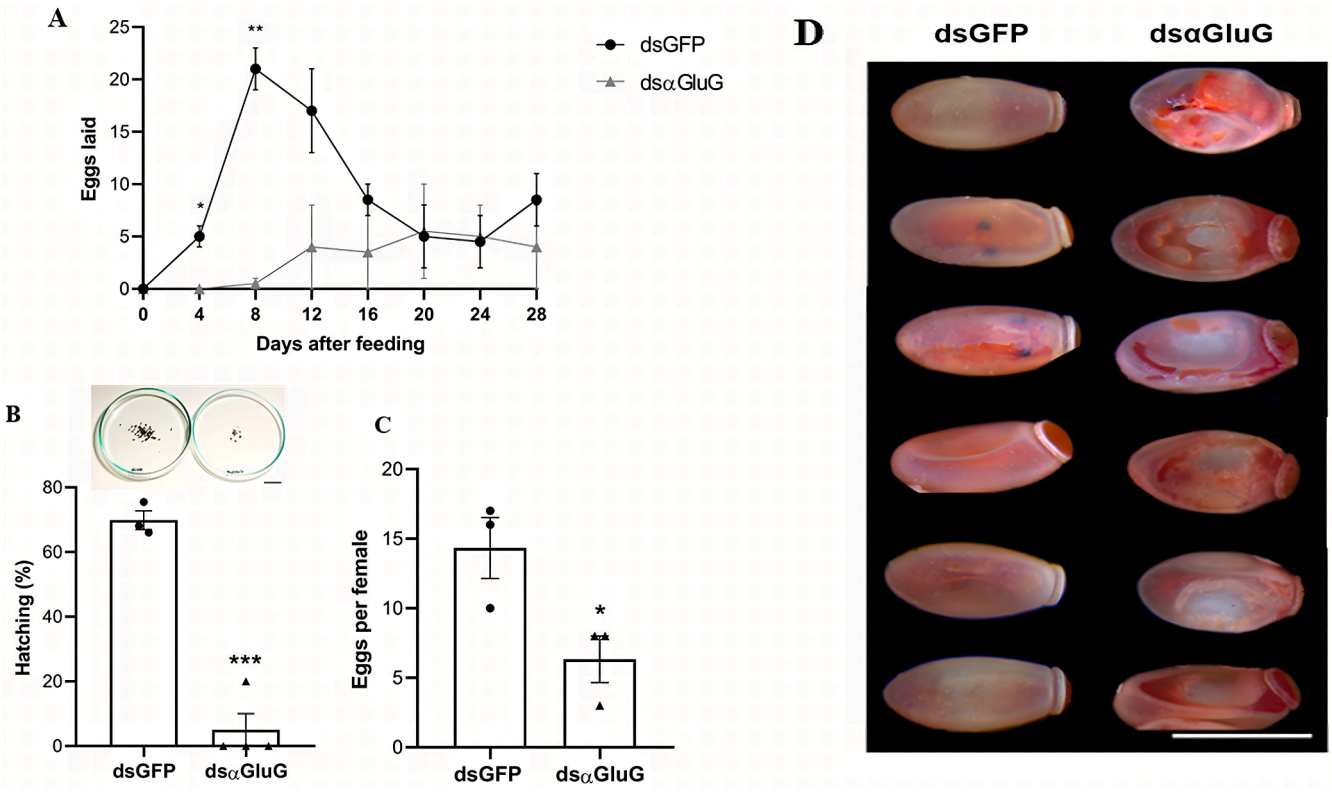

Fig. 4. Analysis of phenotypic changes upon the knockdown of Rp-αGluG. (A) The spatio-temporal distribution reveals a significant reduction in oviposition in females injected with dsαGluG four and eight days after feeding (4 days * $p = 0.0377$; 8 days ** $p = 0.010$; 12 days 0.1483; 16 days 0.3196; 20 days 0.9348; 24 days 0.9098 28 days 0.4408) $n = 10$ per group. Unpaired parametric *t*-test was used for all analyses. (B) After 40 days of feeding, 20 days from the start of hatching with the proportions of dsGFP (left) and dsαGluG (right) groups. Scale bar=1 cm. Percentage of hatched nymphs (dsGFP: 69.8%; dsαGluG: 5%; $p = 0.0002$). (C) Oviposition per female (dsGFP – $n = 14$; dsαGluG – $n = 17$; $p = 0.0437$). Statistical analysis using unpaired *t*-test and expressed with mean and SEM (A-C). (D) Phenotype of the remaining eggs, showing that microinjection with dsαGluG, causes deformations, indicating the occurrence of an abnormal process triggered by metabolic and/or physiological dysfunction. Scale bar = 1mm. dsGFP: females injected with unrelated double strand RNA; dsαGluG: females injected with dsRNA of Rp-αGluG.

and Cerami 1992; Mury et al., 2009; Villiers and Egan 2021). Oliveira et al., (2000), Silva et al. (2007) and Mury et al. (2009) demonstrated either direct or indirectly that α-glucosidases participate in the formation of the Hz biocrystal. Therefore, the secondary function that α-glucosidases acquired in hematophagous hemipterans deserves a more accurate investigation. We used the sequence published by Mury et al. (2009) to decide which isoform would be chosen for the study. After analyzing the complete *R. prolixus* genome and its digestive tract transcriptome (Ribeiro et al., 2014; Mesquita et al., 2015), we identified seven α-glucosidase genes. Therefore, we hypothesize one enzyme encoded by these genes may play a role in the heme detoxification. We conducted a phylogenetic analysis of the α-glucosidase sequences of *R. prolixus* (Fig. 1A). The analysis revealed that isoforms G (RPRC013046) and C (RPRC012963) are more similar to that published by Mury et al. (2009). However, the A isoform is less similar to the G and C isoforms on the phylogenetic tree. The inability of A isoform to affect hemozoin formation may be due to sequence differences that affect the enzyme's structure and function (Fig. 1A and Supplementary Figus. S1 and S6).

Further bioinformatics analysis indicates that the prediction of the amino acid sequence of Rp-αGluG harbors a signal peptide and membrane anchoring sequences (Supplementary Fig. S2). The molecular docking between Rp-αGluG and the heme molecule (Fig. 1B and C) highlights the cavity that holds the heme ligand, containing histidine and aspartic acid residues and representing the same region of interaction with the natural substrate. Previous studies indicate the contribution of these residues in the Hz formation in *Plasmodium vinckei* (Soni et al., 2015) and *P. falciparum* (Nakatani et al., 2014), also in α-glucosidase activity of *E. histolytica* (Bravo-Torres et al., 2004), as well as in Hz formation and α-glucosidase activity in *R. prolixus* (Mury et al., 2009). Furthermore, it has been shown that in a competition assay, prior incubation of α-glucosidase with maltose, a substrate of this enzyme, blocks the formation of Hz, suggesting that these molecules share the same binding site (Mury et al., 2009). Since gene knockdown was confirmed by reduced mRNA expression (Fig. 2A), as well as the enzyme activity was lower (Fig. 2B), it is possible to indicate that the observed effects were caused by dsαGluG. This finding indicates that this isoform is present in the PMMs participating in the heme detoxification process, as reduced Hz formation was detected *in vivo* in adult females challenged with dsαGluG (Fig. 2C). Therefore, these results strongly indicate that this molecule is indeed a biomarker of PMMs that contributes to the heme detoxification mechanism in *R. prolixus*.

Hemoglobin is the most abundant protein found in erythrocytes (Ball et al., 1948; Emadi et al., 2019). Unpublished data from our group show that free heme overload impairs hemoglobin proteolysis *in vitro*, most likely because higher levels of this molecule are associated with reduced digestive enzymes efficiency. Marques et al. (2015) reported an allosteric inhibition of the *P. falciparum* cysteine protease falcipain-2 by free heme. During the preparation of our samples for analysis of H_2O_2 quantification levels, the supernatant of posterior midgut from females injected with dsαGluG was reddish (data not shown), which may indicate a greater accumulation of hemoglobin and/or heme in this area of the gut. Previous studies support our observation as a stronger reddish pigmentation in the hemolymph of females injected with dsαGlu has been observed elsewhere (Mury et al., 2009) as well as in the hemolymph of insects fed with quinoline drug quinidine that blocks Hz

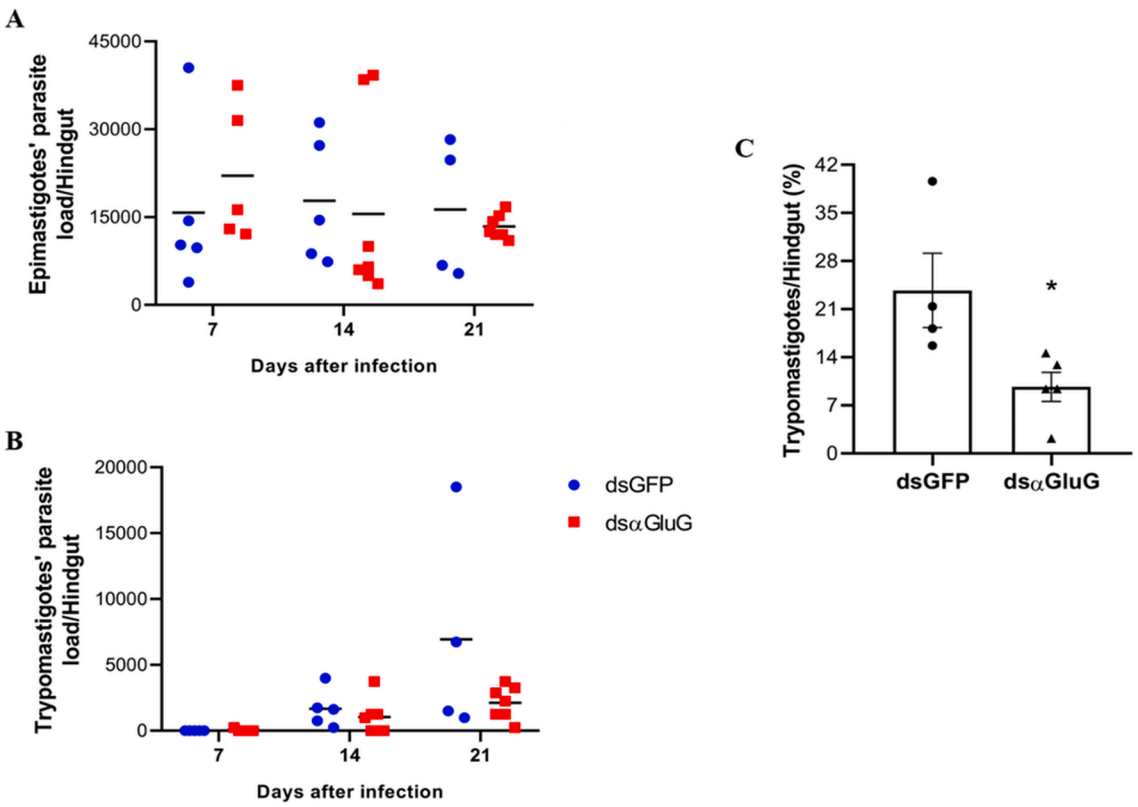

Fig. 5. *T. cruzi* load, (A) Epimastigotes and (B) Metacyclic trypomastigotes. In replicative forms (A), there was a trend toward an increase in parasite load 7 days post infection in the group injected with dsαGluG, compared to dsGFP, but in 14 and 21 days of infection, there was no clear difference. As for the infective forms (B), the most remarkable change was found on the 21st day of analysis, indicating a reduction in the number of this form in the hindgut of dsαGluG females. (seven days: dsGFP – $n = 5$ and dsαGluG – $n = 5$; 14 days: dsGFP – $n = 5$ and dsαGluG – $n = 7$; 21 days: dsGFP – $n = 4$ and dsαGluG – $n = 7$). (C) Rate of metacyclogenesis of *T. cruzi* 21 days after infection. It was assumed that the total number of parasites, counting epimastigotes and trypomastigotes, was 100% and the percentage of trypomastigotes was calculated (dsGFP – $n = 4$ and dsαGluG – $n = 5$;* $p = 0.0340$). Statistical analysis using unpaired *t*-test and expressed with mean and SEM. dsGFP: females injected with unrelated double strand; dsαGluG: females injected with Rp-αGluG.

formation by binding to heme (Ferreira et al., 2018), suggesting increased extravasation of both free heme and hemoglobin, from the gut to the hemolymph. Our results showed the injection of dsαGluG led to an increase of remaining hemoglobin in the anterior midgut, which turns out the knockdown is affecting hemoglobin digestion. Since dsαGluG injection caused a reduction in the levels of Hz formed during blood digestion, it is feasible that an increase of free heme is causing an inhibitory effect on the hemoglobin digestion, as demonstrated for *P. Falciparum* cysteine protease, once blood digestion in *R. prolixus* is accomplished mainly by cysteine protease as well (Henriques et al., 2021).

Mitochondria are organelles known for their crucial role in aerobic metabolism, where ATP synthesis obtained through the proton gradient and the oxidative phosphorylation process constantly produce ROS (Moller, 2001; Vanlerberghe, 2013; Dache and Thierry, 2023). Mitochondrial uncoupling proteins (UCPs) are used to control the ROS level, with the role of protecting against oxidative stress (Maxwell et al., 1999; Brandalise et al., 2003). In *R. prolixus*, both gene expression and protein content of UCP 4 (RpUcp4) are induced after blood feeding while lower H_2O_2 levels were observed (Alves-Bezerra et al., 2014), indicating that this protein plays an important role in protection against oxidative stress. mRNA expression analyses indicate that RpUcp4 is the predominant isoform expressed in anterior midgut (Alves-Bezerra et al., 2014) where the molecule may be assisting in the antioxidant defense process. This activity may happen concomitantly with the detoxification process via heme biocrystallization in the posterior midgut. Upon dsαGluG microinjection, females bugs show increased H_2O_2 formation in the posterior midgut, as quantified, and detected by the fluorescent microscopy. As hypothesized, the reduction in Hz formation and potential accumulation of free heme generates an environment that facilitates the formation of ROS. This effect may propagate a reactive environment in other areas of the gut. In adverse conditions, the action of RpUcp4 may be impaired, leading to formation of ROS in higher quantities in the mitochondria.

Other physiological processes are also triggered by blood feeding such as oogenesis (Buxton, 1930), in which the presence of RHBP bound to the heme molecule in significant amounts (Oliveira et al., 1995), plays an important role in this mechanism. A delay in the spatio-temporal distribution of oviposition was observed in females injected with dsαGluG (Fig. 4A). Additionally, higher levels of remaining hemoglobin were found in the anterior midgut (Fig. 3A), four days after feeding, a period in which delayed oviposition is already observed. Thus, the lower rate of hemoglobin proteolysis by cysteine proteases may negatively affect oviposition, which explains the delay observed. In second reproductive cycle females' oviposition, a compensation phenomenon is observed from the 16th day after feeding, that may be related to the resumption of the digestion, since seven days after feeding this scenario is no longer observed (data not shown). Our data suggest that the process of hemoglobin digestion and subsequent heme release are important for the maintenance of oogenesis.

A smaller number of hatching nymphs was frequent throughout our study, in which less than half of the nymphs in the dsαGluG group hatched, when compared to the control (Fig. 4B). At 40 days after feeding, remaining eggs from females injected with dsαGluG had an abnormal morphology with a non-homogeneous distribution of the egg content (Fig. 4D). A similar phenotype was observed in eggs from

females microinjected with the ferritin double strand molecule (dsFer), which is important in heme and iron metabolism. Eggs displayed a morphology very similar to what we have seen, and according to these authors, the abnormal morphology may be induced by dehydration (Walter-Nuno et al., 2018).

Even though heme is an important element for embryogenesis when properly associated to the RHBP in the oocytes (Braz et al., 2002; Atella et al., 2005), the reduction observed in oviposition may be related to the impact of higher free heme after reduction in Hz formation, which may have impaired embryonic development due to redox imbalance (Ferreira et al., 2018). On the other hand, the reduced hatching of nymphs from the group injected with dsαGluG suggests the action of the parental RNAi on the offspring (Fig. 4B). We have not observed the same phenotype when performing the same experiments with females at the second reproductive cycle (data not shown). The response to exogenous RNAi (exo-RNAi) varies according to the species (Bellés, 2010). In the *Caenorhabditis elegans* model, exo-RNA led to systemic effects that triggered a parental effect of RNAi (Winston et al., 2002). In *R. prolixus*, microinjection into 5th stage nymphs was shown to have an effect that lasted up to 2nd stage nymphs of the F1 generation, indicating the persistence of dsRNA (Paim et al., 2013b). Yet, in studies with this triatomine, it has been seen that the knockdown of genes related to heme and iron metabolism induced increased mortality of adults and 1st stage nymphs after feeding, in addition to reduced ecdysis of the latter group (Walter-Nuno et al., 2018). In our experiments, the nymphs showed a higher mortality rate even before a blood meal, supporting the hypothesis of the parental effect of dsαGluG, with more detrimental consequences on offspring survival.

After taking an infected blood meal from a vertebrate host, the *T. cruzi* parasite develops exclusively in the midgut of Triatominae. Throughout parasite-host coevolution, *T. cruzi* developed strategies to escape the intense hemoglobin hydrolysis in the anterior midgut and to take advantage of products derived from blood digestion to fulfill proliferation in the posterior midgut, and metacyclogenesis in the hindgut. Nogueira et al. (2017) showed that heme-induced mitochondrial ROS favors the proliferation of *T. cruzi* epimastigotes forms. Ferreira et al. (2018) reported that the drug quinidine, that forms a stable complex with heme, impairs Hz formation in the midgut lumen of *R. prolixus*.

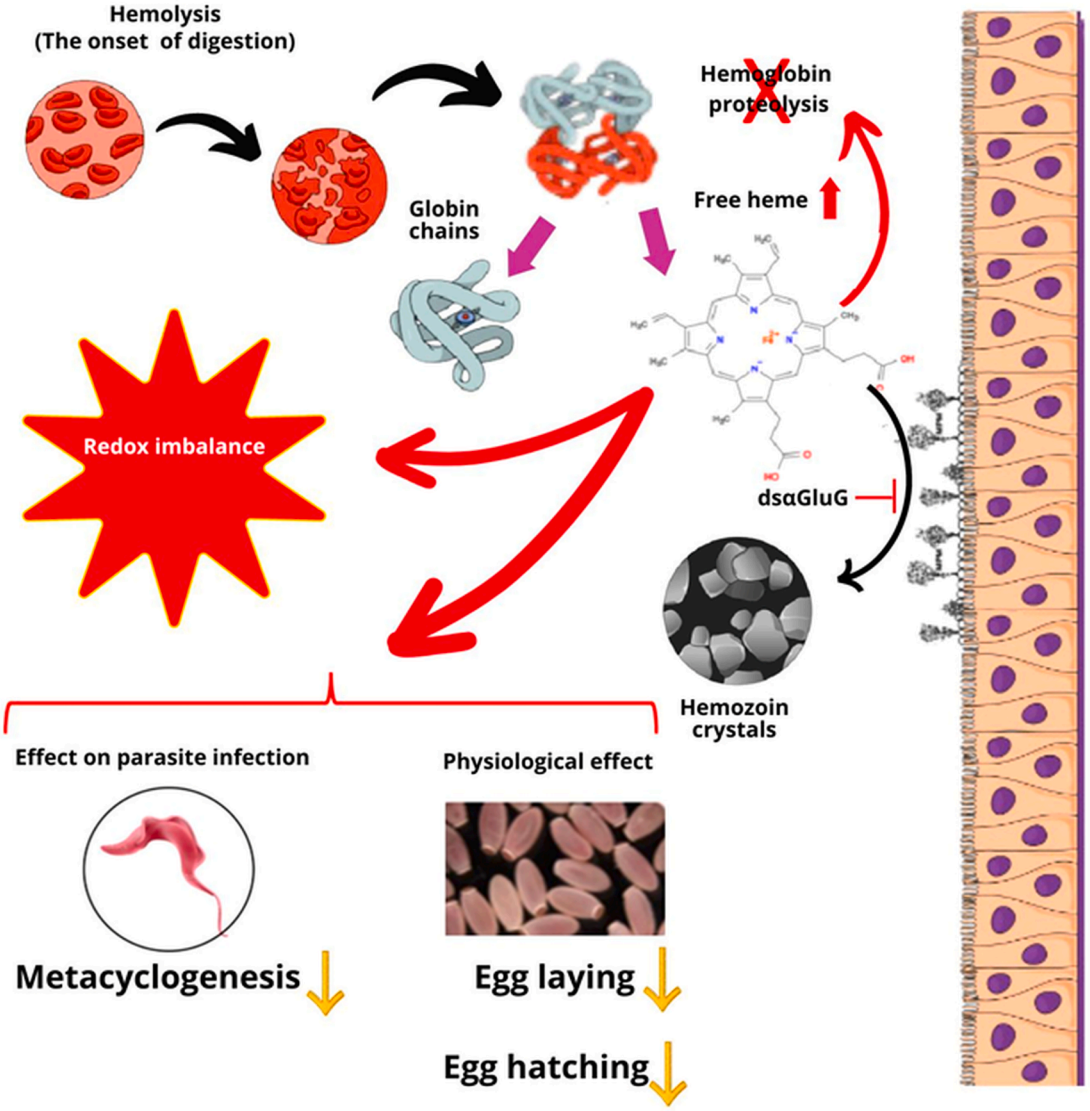

Fig. 6. Summary of effects based on Rp-αGluG knockdown. After dsRNA treatment, impairment to hemozoin biocrystallization was observed, resulting in higher levels of H_2O_2 in the posterior midgut. The buildup of free heme affects hemoglobin digestion, delay oviposition, reduce hatching and caused morphological changes in eggs. For the *T. cruzi* establishment, knockdown of αGluG leads to heme overload, what has a positive influence on proliferation, but provide a detrimental environment for metacyclogenesis.

Furthermore, they noticed that non-biocrystallized heme accumulated in the midgut induced cytotoxic effects for the *T. cruzi*. The evolutionary forms of *T. cruzi* that complete their life cycle in the gut of this vector require distinct environments for their development. The replicative forms, epimastigotes, depend on the most oxidative environment to replicate in the posterior midgut, which is triggered by the presence of heme. For the metacyclic trypomastigotes, which are the infectious forms, their differentiation occurs in the hindgut, which is a more reducing and nutrient-poor environment (Nogueira et al., 2011; Nogueira et al., 2015; Nogueira et al., 2017).

It has been shown that a pro-oxidant environment plays an important role in the proliferation of epimastigote forms, as shown by treatment with pro-oxidant molecules *in vitro* (Nogueira et al., 2015). In the present work, levels of epimastigote forms suggest an increase at 7 days after infection of females injected with dsαGluG (Fig. 5A). These data indicate that the replicative forms of *T. cruzi* develop better in a pro-oxidant environment, since they are found in higher quantities in the rectum of females injected with dsαGluG. Thus, dsαGluG, by triggering a reduction in Hz formation, would probably be causing an overload of free heme, which may be favoring the maintenance of epimastigote proliferation in a pro-oxidant environment. In addition, Nogueira et al. (2015) demonstrated that infection of *R. prolixus* nymphs with *T. cruzi* supplemented with antioxidant molecules was associated with significantly higher levels of metacyclic trypomastigotes in the three segments of the gut (anterior and posterior midgut, and rectum), indicating that a less oxidative environment favors *T. cruzi* metacyclogenesis. Upon microinjection with dsαGluG, fewer trypomastigotes, 14 and 21 days post infection (Fig. 5B), is a strong indication that the oxidative scenario caused by knockdown of αGluG is impairing metacyclogenesis (Fig. 5C).

Additionally, Garcia et al. (1995) showed that hemoglobin-derived proteins present in the blood, during digestion, modulate the differentiation of *T. cruzi* in the intestinal tract of *R. prolixus*, with contribution of peptides corresponding to fragments of hemoglobin, the αD-globin. Thus, the possibility of a shortage of hemoglobin fragments, marked by a delay in the digestion of this molecule, as demonstrated by dsαGluG, may also be an additional limiting factor that explains the presence of fewer trypomastigotes in females microinjected with dsαGluG.

5. Conclusion

Herein we provide evidence that Rp-αGluG is important in Hz formation, an important mechanism of heme detoxification. However, it remains to be shown whether other isoforms also play a role in the heme detoxification process in this organism. The identity of each isoform, as well as which of them are involved in this process remains unknown. Additionally, the contribution of the G isoform in the metacyclogenesis of the *T. cruzi* parasite has been reported for the first time.

The knockdown of Rp-αGluG lead to a gene expression that was significantly lower compared to the control, but the activity of membrane-specific α-glucosidases was not proportional to the lower level of the α-GluG gene knockdown. This fact supports the idea that other α-glucosidases might be involved with heme detoxification, otherwise we should have seen a drastic fall in enzyme activity. Here we were unable to specifically define the activity of Rp-αGluG and how much of it is functionally abundant in PMMs. Lastly, it is still necessary to explore how Rp-αGluG interacts with the other isoforms.

We were also able to show the negative impact of knockdown of αGluG on egg laying and hatching, even though further studies may be important to understand the impact of dsαGluG on biochemical and physiological parameters during digestion as well as other components associated with oxidative homeostasis and defense systems (Fig. 6). Whether the build-up of free heme impacts the cellular architecture of the intestinal epithelium should also be further investigated.

Funding sources

This work was supported by grants from the Fundação de Amparo à Pesquisa do Estado do Rio de Janeiro (FAPERJ, E-26/210.119/2022 and E-26/210.708/2021). FFM was supported by post-graduate fellowship from FAPERJ (E-26/201.050/2020). C.A. was a PhD student of PPG-PRODBIO-Macaé (Coordenação de Aperfeiçoamento de Pessoal de Nível Superior - CAPES scholarship).

CRediT authorship contribution statement

Fernanda Ferreira Maissner: Conceptualization, Methodology, Validation, Formal analysis, Investigation, Resources, Writing – original draft, Writing – review & editing, Visualization. **Carina Azevedo Oliveira Silva:** Methodology, Validation, Formal analysis, Investigation, Resources, Writing – original draft, Visualization. **André Borges Farias:** Methodology, Resources, Visualization. **Evenilton Pessoa Costa:** Methodology, Resources, Visualization, Writing – review & editing. **José Luciano Nepomuceno-Silva:** Methodology, Resources, Writing – review & editing, Funding acquisition. **José Roberto da Silva:** Conceptualization, Validation, Resources, Writing – review & editing, Funding acquisition. **Flávia Borges Mury:** Conceptualization, Validation, Investigation, Resources, Supervision, Writing – review & editing, Visualization, Funding acquisition.

Declaration of competing interest

The authors declare that they have no known competing financial interests or personal relationships that could have appeared to influence the work reported in this paper.

Acknowledgements

We would like to thank members of the Nunes da Fonseca Lab for helpful discussions. We are grateful the José Lima Junior and Simone Azevedo Gomes for technical assistance on the laboratory. We are grateful to the animal facility at the Institute of Biodiversity and Sustentability for technical assistance with *Rhodnius* husbandry.

Supplementary materials

Supplementary material associated with this article can be found, in the online version, at doi:10.1016/j.cris.2024.100100.

Data availability

Data will be made available on request.

References

Aft, R.L., Mueller, G.C., 1983. Hemin-mediated DNA strand scission. J. Biol. Chem. 258, 12069–12072.

Alves-Bezerra, M., Cosentino-Gomes, D., Vieira, L.P., Rocco-Machado, N., Gondim, K.C., Meyer-Fernandes, J.R., 2014. Identification of uncoupling protein 4 from the blood-sucking insect *Rhodnius prolixus* and its possible role on protection against oxidative stress. Insect Biochem. Mol. Biol. 50, 24–33. https://doi.org/10.1016/j.ibmb.2014.03.011.

Atella, G.C., Gondim, K.C, Machado, E.A., Medeiros, M.N., Silva-Netom, M.A.C., Masuda, H., 2005. Oogenesis and egg development in triatomines: a biochemical approach. An. Acad. Bras. De Cienc. 77, 405–430. https://doi.org/10.1590/s0001-37652005000300005.

Azambuja, P., Garcia, E.S., 1997. Care and maintenance of triatomine colonies. In: Crampton, J.M., Beard, C.B., Louis, C. (Eds.), The Molecular Biology of Insect Disease Vectors. Springer, Dordrecht, pp. 56–66. https://doi.org/10.1007/978-94-009-1535-0_6.

Ball, E.G., McKee, R.W., Anfinsen, C.B., Cruz, W.O., Geiman, Q.M., 1948. Studies on malarial parasites: chemical and metabolic changes during growth and multiplication *in vivo* and *in vitro*. J. Biol. Chem. 175, 547–571.

Bellés, X., 2010. Beyond *Drosophila*: rNAi *in vivo* and functional genomics in insects. Annu Rev. Entomol. 55, 111–128. https://doi.org/10.1146/annurev-ento-112408-085301.

Bern, C., 2015. Chagas' Disease. New Engl. J. Med. 373, 456–466. https://doi.org/10.1056/NEJMra1410150.
Brandalise, M., Maia, I.G., Borecky, J., Vercesi, A.E., Arruda, P., 2003. ZmPUMP encodes a maize mitochondrial uncoupling protein that is induced by oxidative stress. Plant Sci. 165, 329–335. https://doi.org/10.1016/S0168-9452(03)00159-6.
Bravo-Torres, J.C., Villagómez-Castro, J.C., Calvo-Méndez, C., Flores-Carreón, A., López-Romero, E., 2004. Purification and biochemical characterisation of a membrane-bound α-glucosidase from the parasite *Entamoeba histolytica*. Int. J. Parasitol. 34, 455–462. https://doi.org/10.1016/j.ijpara.2003.11.015.
Braz, G.R.C., Moreira, M.F., Masuda, H., Oliveira, P.L., 2002. *Rhodnius* heme-binding protein (RHBP) is a heme source for embryonic development in the blood-sucking bug *Rhodnius prolixus* (Hemiptera: reduviidae). Insect Biochem. Mol. Biol. 32, 361–367. https://doi.org/10.1016/s0965-1748(01)00163-1.
Buxton, P.A., 1930. The biology of a blood-sucking bug, *Rhodnius prolixus*. Trans. Ent. Soc. 78, 227–236. https://doi.org/10.1111/j.1365-2311.1930.tb00385.x.
Dache, Z.A.A., Thierry, A.R., 2023. Mitochondria-derived cell-to-cell communication. Cell Rep. 42, 112728. https://doi.org/10.1016/j.celrep.2023.112728.
Dansa-Petretski, M., Ribeiro, J.M., Atella, G.C., Masuda, H., Oliveira, P.L., 1995. Antioxidant role of *Rhodnius prolixus* heme-binding protein. Protection against heme-induced lipid peroxidation. J. Biol. Chem. 270, 10893–10896. https://doi.org/10.1074/jbc.270.18.10893.
DNDI – Neglected Diseases Initiative. 2023. Chagas disease: symptoms, transmission, and current treatments for Chagas disease. Avaialable on: https://dndi.org/diseases/chagas/facts/?gclid=CjwKCAiAu5agBhBzEiwAdiR5tFyn46EIH26lAMNlh1Sl9WevDp5VJ2NAt3E3EA6E2o07KySFJ0Rg4xoCwNsQAvD_BwE.
Emadi, M., Maghami, P., Khorsandi, K., Hosseinzadeh, R., 2019. Biophysical study on the interaction of cartap hydrochloride and hemoglobin: heme degradation and functional changes of protein. J. Biochem. Mol. Toxicol. 33, 1–8. https://doi.org/10.1002/jbt.22325.
Ferreira, C.M., Stiebler, R., Saraiva, F.M., Lechuga, G.C., Walter-Nuno, A.B., Bourguignon, S.C., Gonzalez, M.S., Azambuja, P., Gandara, A.C.P., Menna-Barreto, R.F.S., Paiva-Silva, G.O., Paes, M.C., Oliveira, M.F., 2018. Heme crystallization in a Chagas disease vector acts as a redox-protective mechanism to allow insect reproduction and parasite infection. PLoS Negl. Trop. Dis. 12, e0006661. https://doi.org/10.1371/journal.pntd.0006661, 1–20.
Ferreira, R.C., Kessler, R.L., Lorenzo, M.G., Paim, R.M., Ferreira, L, de, L., Probst, C.M., Alves-Silva, J., Guarneri, A.A., 2016. Colonization of *Rhodnius prolixus* gut by *Trypanosoma cruzi* involves an extensive parasite killing. Parasitology 143 (4), 434–443. https://doi.org/10.1017/S0031182015001857. AprEpub 2016 Jan 28. PMID: 26818093.
Frisch, M.J., Trucks, G.W., Schlegel, H.B., Scuseria, G.E., Robb, M.A., Cheeseman, J.R., Montgomery Jr, J.A., Vreven, T., Kudin, K.N., Burant, J.C., Millam, J.M., Iyengar, S. S., Tomasi, J., Barone, V., Mennucci, B., Cossi, M., Scalmani, G., Rega, N., Petersson, G.A., Nakatsuji, H., Hada, M., Ehara, M., Toyota, K., Fukuda, R., Hasegawa, J., Ishida, M., Nakajima, T., Honda, Y., Kitao, O., Nakai, H., Klene, M., Li, X., Knox, J.E., Hratchian, H.P., Cross, J.B., Bakken, V., Adamo, C., Jaramillo, J., Gomperts, R., Stratmann, R.E., Yazyev, O., Austin, A.J., Cammi, R., Pomelli, C., Ochterski, J.W., Ayala, P.Y., Morokuma, K., Voth, G.A., Salvador, P., Dannenberg, J. J., Zakrzewski, V.G., Dapprich, S., Daniels, A.D., Strain, M.C., Farkas, O., Malick, D. K., Rabuck, A.D., Raghavachari, K., Foresman, J.B., Ortiz, J.V., Cui, Q., Baboul, A.G., Clifford, S., Cioslowski, J., Stefanov, B.B., Liu, G., Liashenko, A., Piskorz, P., Komaromi, I., Martin, R.L., Fox, D.J., Keith, T., Al-Laham, M.A., Peng, C.Y., Nanayakkara, A., Challacombe, M., Gill, P.M.W., Johnson, B., Chen, W., Wong, M. W., Gonzalez, C., Pople, J.A., 2004. Gaussian, Inc. Wallingford CT. https://gaussian.com/g03citation/.
Gama, M.V.F., Moraes, C.S., Gomes, B., Diaz-Albiter, H.M., Mesquita, R.D., Seabra-Junior, E., Azambuja, P., Garcia, E.S., Genta, F.A., 2022. Structure and expression of *Rhodnius prolixus* GH18 chitinases and chitinase-like proteins: characterization of the physiological role of RpCht7, a gene from subgroup VIII, in vector fitness and reproduction. Front. Physiol. 3 (13), 861620. https://doi.org/10.3389/fphys.2022.861620.eCollection2022.
Garcia, E.S., Gonzalez, M.S., Azambuja, P., Baralle, F.E., Fraidenraich, D., Torres, H.N., Flawiá, M.M., 1995. Induction of *Trypanosoma cruzi* metacyclogenesis in the gut. Exp. Parasitol. 81, 255–261. https://doi.org/10.1006/expr.1995.1116.
Graça-Souza, A.V., Maya-Monteiro, C., Paiva-Silva, G.O., Braz, G.R.C., Paes, M.C., Sorgine, M.H.F., Oliveira, M.F., Oliveira, P.L., 2006. Adaptations against heme toxicity in blood-feeding arthropods. Insect Biochem. Mol. Biol. 36, 322–335. https://doi.org/10.1016/j.ibmb.2006.01.009.
Guarner, J., 2019. Chagas disease as example of a reemerging parasite. Semin. Diagn. Pathol. 36, 164–169. https://doi.org/10.1053/j.semdp.2019.04.008.
Guarneri, A., 2020. Infecting Triatomines with Trypanosomes. Method. Mol. Biol. 69–79, 2020. https://doi.org/10.1007/978-1-0716-0294-2_5.
Gutteridge, J.M.C., Smith, A., 1988. Antioxidant protection by haemopexin of haem-stimulated lipid peroxidation. Biochem. J. 256, 861–865. https://doi.org/10.1042/bj2560861.
Henriques, B.S., Gomes, B., Oliveira, P.L., Garcia, E.S., Azambuja, P., Genta, F.A., 2021. Characterization of the temporal pattern of blood protein digestion in *Rhodnius prolixus*: first description of early and late gut cathepsins. Front. Physiol. 11, 509310. https://doi.org/10.3389/fphys.2020.509310.
Iglesias-Rus, L., Romay-Barja, M., Boquete, T., Benito, A., Blasco-Hernández, T., 2019. The role of the first level of health care in the approach to Chagas disease in a non-endemic country. PLoS Negl. Trop. Dis. 13, e0007937. https://doi.org/10.1371/journal.pntd.0007937.
Jones, G., Willett, P., Glen, R.C., Leach, A.R., Taylor, R., 1997. Development and validation of a genetic algorithm for flexible docking. J. Mol. Biol. 267, 727–748. https://doi.org/10.1006/jmbi.1996.0897.
Justi, S.A., Galvão, C., 2017. The evolutionary origin of diversity in chagas disease vectors. Trend. Parasitol. 33 (1), 42–52. https://doi.org/10.1016/j.pt.2016.11.002.
Kollien, A.H., Schaub, G.A., 1999. Development of *Trypanosoma cruzi* after starvation and feeding of the vector–a review. Tokai J. Exp. Clin. Med. 23, 335–340.
Laskowski, R.A., MacArthur, M.W., Moss, D.S., Thornton, J.M., 1993. PROCHECK: a program to check the stereochemical quality of protein structures. J. Appl. Crystallogr. 26 (2), 283–291. https://doi.org/10.1107/s0021889892009944.
Lehane, M.J., 2005. The Biology of Blood-Sucking in Insects. Cambridge University Press. https://doi.org/10.1017/CBO9780511610493.
Majerowicz, D., Alves-Bezerra, M., Logullo, R., Fonseca-de-Souza, A.L., Meyer-Fernandes, J.R., Braz, G.R., Gondim, K.C., 2011. Looking for reference genes for real-time quantitative PCR experiments in *Rhodnius prolixus* (Hemiptera: reduviidae). Insect. Mol. Biol. 20, 713–722. https://doi.org/10.1111/j.1365-2583.2011.01101.x.
Marques, A.F., Gomes, P.S., Oliveira, P.L., Rosenthal, P.J., Pascutti, P.G., Lima, L.M., 2015. Allosteric regulation of the *Plasmodium falciparum* cysteine protease falcipain-2 by heme. Arch. Biochem. Biophys. 573, 92–99. https://doi.org/10.1016/j.abb.2015.03.007, 2015 May 1Epub 2015 Mar 16. PMID: 25791019.
Maxwell, D.P., Wang, Y., McIntosh, L., 1999. The alternative oxidase lowers mitochondrial reactive oxygen production in plant cells. Proc. Natl. Acad. Sci. USA 96, 8271–8276. https://doi.org/10.1073/pnas.96.14.8271.
Melo, R.F.P., Guarneri, A.A., Silber, A.M., 2020. The influence of environmental cues on the development of *Trypanosoma cruzi* in triatominae vector. Front. Cell Infect. Microbiol. 10. https://doi.org/10.3389/fcimb.2020.00027.
Mesquita, R.D., Vionette-Amaral, R.J., Lowenberger, C., Rivera-Pomar, R., Monteiro, F. A., Minx, P., Spieth, J., Carvalho, A.B., Panzera, F., Lawson, D., Torres, A.Q., Ribeiro, J.M.C., Sorgine, M.H.F, Waterhouse, R.M., Montague, M.J., Abad-Franch, F., Alves-Bezerra, M., Amaral, L.R., Araujo, H.M., Araujo, R.N., Aravind, L., Atella, G.C., Azambuja, P., Berni, M., Bittencourt-Cunha, P.R., Braz, G.R.C., Calderón-Fernández, G., Cararetto, C.M.A., Christensen, M.B., Costa, I.R., Costa, S.G., Dansa, M., Daumas-Filho, C.R.O., De-Paula, I.F., Dias, F.A., Dimopoulos, G., Emrich, S.J., Esponda-Behrens, N., Fampa, P., Fernandez-Medina, R.D., Fonseca, R. N., Fontenele, M., Fronick, C., Fulton, L.A., Gandara, A.C., Garcia, E.S., Genta, F.A., Giraldo-Calderón, G.I., Gomes, B., Gondim, K.C., Granzotto, A., Guarneri, A.A., Guigó, R., Harry, M., Hughes, D.S.T., Jablonka, W., Jacquin-Joly, E., Juárez, M.P., Koerich, L.B., Lange, A.B., Latorre-Estivalis, J.M, Lavore, A., Lawrence, G.G., Lazoski, C., Lazzari, C.R., Lopes, R.R., Lorenzo, M.G., Lugon, M.D., Majerowicz, D., Marcet, P.L., Mariotti, M., Masuda, H., Megy, K., Melo, A.C.A., Missirlis, F., Mota, T., Noriega, F.G., Nouzova, M., Nunes, R.D., Oliveira, R.L.L., Oliveira-Silveira, G., Ons, S., Orchard, I., Pagola, L., Paiva-Silva, G.O., Pascual, A., Pavan, M.G., Pedrini, N., Peixoto, A.A., Pereira, M.H., Pike, A., Polycarpo, C., Prosdocimi, F., Ribeiro-Rodrigues, R., Robertson, H.M., Salerno, A.P., Salmon, D., Santesmasses, D., Schama, R., Seabra-Junior, E.S., Silva-Cardoso, L., Silva- Neto, M.A.C., Souza-Gomes, M., Sterkel, M., Taracena, M.L., Tojo, M., Tu, Z.J., Tubio, J.M.C., Ursic-Bedoya, R., Venancio, T.M., Walter-Nuno, A.B., Wilson, D., Warren, WC., Wilson, R. K., Huebner, E., Dotson, E.M., Oliveira, P.L., 2015. Genome of *Rhodnius prolixus*, an insect vector of Chagas disease, reveals unique adaptations to hematophagy and parasite infection. Proc. Natl. Acad. Sci. U.S.A. 112, 14936–14941. Epub 2015 Nov 16. Erratum in:Proc Natl Acad Sci U S A. 2016 Mar 8;113(10):E1415-6. Lange, Angela B [added]; Orchard, Ian [added]. PMID: 26627243; PMCID: PMC4672799. 10.1073/pnas.1506226112.
Mills, R.M., 2020. Chagas disease: epidemiology and barriers to treatment. Am. J. Med. 133, 1262–1265. https://doi.org/10.1016/j.amjmed.2020.05.022.
Mittler, R., 2002. Oxidative stress, antioxidants and stress tolerance. Trend. Plant. Sci. 7, 405–410. https://doi.org/10.1016/s1360-1385(02)02312-9.
Miyazaki, T., Park, E.Y., 2020. Structure–function analysis of silkworm sucrose hydrolase uncovers the mechanism of substrate specificity in GH13 subfamily 17 exo-α-glucosidases. J. Biol. Chem. 295 (26), 8784–8797. https://doi.org/10.1074/jbc.ra120.013595 v.n.jun. 2020.
Moller, I.M., 2001. Plant mitochondria and oxidative stress: electron transport, NADPH turnover, and metabolism of reactive oxygen species. Annu. Rev. Plant Physiol. Plant Mol. Biol. 52, 561–591. https://doi.org/10.1146/annurev.arplant.52.1.561.
Mury, F.B., Silva, J.R., Ferreira, L.S., Ferreira, B.S., Souza-Filho, G.A., Souza-Neto, J.A., Ribolla, P.E.M., Silva, C.P., Nascimento, V.V., Machado, O.L.T., Berbert-Molina, M. A., Dansa-Petretski, M., 2009. Alpha-glucosidase promotes hemozoin formation in a blood-sucking bug: an evolutionary history. PLoS ONE 4, e6966. https://doi.org/10.1371/journal.pone.0006966.
Nakatani, K., Ishikawa, H., Aono, S., Mizutani, Y., 2014. Identification of essential histidine residues involved in heme binding and hemozoin formation in heme detoxification protein from Plasmodium falciparum. Sci. Rep. 4, 1–7. https://doi.org/10.1038/srep06137.
Nogueira, N.P., Saraiva, F.M.S., Oliveira, M.P., Mendonça, A.P.M., Inacio, J.D.F., Almeida-Amaral, E.E., Menna-Barreto, R.F., Laranja, G.A.T., Torres, E.J.L., Oliveira, M.F., Paes, M.C., 2017. Heme modulates *Trypanosoma cruzi* bioenergetics inducing mitochondrial ROS production. Free Radic. Biol. Med. 108, 183–191. https://doi.org/10.1016/j.freeradbiomed.2017.03.027.
Nogueira, N.P., Saraiva, F.M.S., Sultano, P.E., Cunha, P.R.B.B., Laranja, G.A.T., Justo, G. A., Sabino, K.C.C., Coelho, M.G.P., Rossini, A., Atella, G.C., Paes, M.C., 2015. Proliferation and differentiation of *Trypanosoma cruzi* inside its vector have a new trigger: redox status. PLoS ONE 10, e0116712. https://doi.org/10.1371/journal.pone.0116712.
Nogueira, N.P.A., Souza, C.F., Saraiva, F.M.S., Sultano, P.E., Dalmau, S.R., Bruno, R.E., Gonçalves, R.L.S., Laranja, G.A.T., Leal, L.H.M., Coelho, M.G.P., Masuda, C.A., Oliveira, M.F., Paes, M.C., 2011. Heme-induced ROS in *Trypanosoma cruzi* activates CaMKII- like that triggers epimastigote proliferation. one helpful effect of ROS. PLoS ONE 6, e25935. https://doi.org/10.1371/journal.pone.0025935.

Oliveira, M.F., D'Avila, J.C., Torres, C.R., Oliveira, PL., Tempone, A.J., Rumjanek, F.D., Braga, C.M., Silva, J.R., Dansa-Petrestki, M., Oliveira, M.A., Souza, W., Ferreira, S.T., 2000. Haemozoin in *Schistosoma mansoni*. Mol. Biochem. Parasitol. 111, 217–221. https://doi.org/10.1016/s0166-6851(00)00299-1.

Oliveira, M.F., Silva, J.R., Dansa-Petrestki, M., Souza, W., Lins, U., Braga, C.M., Masuda, H., Oliveira, P.L., 1999. Haem detoxification by an insect. Nature 400, 517–518. https://doi.org/10.1038/22910.

Oliveira, M.F., Timm, B.L., Machado, E.A., Miranda, K., Attias, M., Silva, J.R., Dansa-Petrestki, M., Oliveira, M.A., Souza, W., Pinhal, N.M., Sousa, J.J.F., Vugman, N.V., Oliveira, P.L., 2002. On the pro-oxidant effects of haemozoin. FEBS Lett. 512, 139–144. https://doi.org/10.1016/s0014-5793(02)02243-3.

Oliveira, P.L., Kawooya, J.K., Ribeiro, J.M., Meyer, T., Poorman, R., Alves, E.W., Walker, F.A., Machado, E.A., Nussenzveig, R.H., Padovan, G.J., Masuda, H., 1995. A heme-binding protein from hemolymph and oocytes of the blood- sucking insect, *Rhodnius prolixus*. Isolation and characterization. J. Biol. Chem. 270, 10897–10901. https://doi.org/10.1074/jbc.270.18.10897.

Paes, M.C., Oliveira, M.B., Oliveira, P.L., 2001. Hydrogen peroxide detoxification in the midgut of the blood-sucking insect, *Rhodnius prolixus*. Arch. Insect Biochem. Physiol. 48, 63–71. https://doi.org/10.1002/arch.1058.

Paes, M.C., Oliveira, P.L., 1999. Extracellular glutathione peroxidase from the blood-sucking bug, *Rhodnius prolixus*. Arch. Insect Biochem. Physiol. 41, 171–177. https://doi.org/10.1002/(SICI)1520-6327(1999)41:4<171::AID-ARCH1>3.0.CO;2-5.

Paim, R.M.M., Araujo, R.N., Lehane, M.J., Gontijo, N.F., Pereira, M.H., 2013a. Application of RNA interference in triatomine (Hemiptera:reduviidae) studies. Insect Sci. 20, 40–52. https://doi.org/10.1111/j.1744-7917.2012.01540.x.

Paim, R.M.M., Araujo, R.N., Lehane, M.J., Gontijo, N.F., Pereira, M.H., 2013b. Long-term effects and parental RNAi in the blood feeder *Rhodnius prolixus* (Hemiptera; Reduviidae). Insect Biochem. Mol. Biol. 43, 1015–1020. https://doi.org/10.1016/j.ibmb.2013.08.008.

Pascual, A., Vilardo, E.S., Taibo, C., García, J.S., Pomar, R., 2021. Bicaudal C is required for the function of the follicular epithelium during oogenesis in *Rhodnius prolixus*. Dev. Gene. Evol. 231, 33–45. https://doi.org/10.1007/s00427-021-00673-0.

Patel, P., 2020. Chagas disease: quick facts. Nursing (Brux) 50, 13–15. https://doi.org/10.1097/01.NURSE.0000694824.61152.89.

Pérez-Molina, J.A., Molina, I., 2018. Chagas disease. Lancet 391, 82–94. https://doi.org/10.1016/S0140-6736(17)31612-4.

Ribeiro, J.M.C., Genta, F.A., Sorgine, M.H.F., Logullo, R., Mesquita, R.D., Paiva-Silva, G. O., Majerowicz, D., Medeiros, M., Koerich, L., Terra, W.R., Ferreira, C., Pimentel, A. C., Bisch, P.M., Leite, D.C., Diniz, M.M.P., Junior, J.L.S.G.V., Silva, M.L., Araujo, R. N., Gandara, A.C.P., Brosson, S., Salmon, D., Boubsata, S., González-Caballero, Silber, A.M., Alves-Bezerra, M., Gondim, K.C., Silva-Neto, M.A.C., Atella, G.C., Araujo, H., Dias, F.A., Polycarpo, C., Vionette. Amaral, R.J., Fampa, P., Melo, A.C.A., Tanaka, A.S., Balczun, C., Oliveira, J.H.M., Gonçalves, R.L.S., Lazoski, C., Rivera-Pomar, R., Diambra, L., Schaub, G.A., Garcia, E.S., Azambuja, P., Braz, G.R.C., Oliveira, P.L., 2014. An insight into the transcriptome of the digestive tract of the bloodsucking bug, *Rhodnius prolixus*. PLoS Negl. Trop. Dis. 8, 27. https://doi.org/10.1371/journal.pntd.0002594.

Ryter, S.W., Tyrrell, R.M., 2000. The heme synthesis and degradation pathways: role in oxidant sensitivity Heme oxygenase has both pro- and antioxidant properties. Free Radic. Biol. Med. 28, 289–309. https://doi.org/10.1016/s0891-5849(99)00223-3.

Schmitt, T., Frezzatti, W., Schreier, S., 1993. Hemin-induced lipid membrane disorder and increased permeability. Arch. Biochem Biophys. 307, 96–103. https://doi.org/10.1006/abbi.1993.1566.

Schofield, C.J., Galvão, C., 2009. Classification, evolution and species groups within the Triatominae. Acta Trop. 110, 88–100. https://doi.org/10.1016/j.actatropica.2009.01.010.

Schrodinger, L., 2015. The PyMOL Molecular Graphics System. Version 2.4.0a0 2010, 1 (5), 0.

Shimizu, T., Lengalova, A., Martínek, V., Martínková, M., 2019. Heme: emergent roles of heme in signal transduction, functional regulation and as catalytic centres. Chem. Soc. Rev. 48, 5624–5657. https://doi.org/10.1039/c9cs00268e.

Silva, C.P., Ribeiro, A.F., Gulbenkian, S., Terra, W.R., 1995. Organization, origin and function of the outer microvillar (perimicrovillar) membranes of *Dysdercus peruvianus* (Hemiptera) midgut cells. J. Insect Physiol. 41, 1093–1103. https://doi.org/10.1016/0022-1910(95)00066-4.

Silva, C.P., Silva, J.R., Vasconcelos, F.F., Petrestki, M.D.A., Damatta, R.A., Ribeiro, A.F., Terra, W.R., 2004. Occurrence of midgut perimicrovillar membranes in paraneopteran insect orders with comments on their function and evolutionary significance. Arthropod. Struct. Dev. 33, 139–148. https://doi.org/10.1016/j.asd.2003.12.002.

Silva, J.R., Gomes-Silva, L., Lins, U.C., Nogueira, N.F.S., Dansa-Petretski, M., 2006. The haemoxisome: a haem-iron containing structure in the *Rhodnius prolixus* midgut cells. J. Insect Physiol. 52, 542–550. https://doi.org/10.1016/j.jinsphys.2006.01.004.

Silva, J.R., Mury, F.B., Oliveira, M.F., Oliveira, P.L., Silva, C.P., Dansa-Petretski, M., 2007. Perimicrovillar membranes promote hemozoin formation into *Rhodnius prolixus* midgut. Insect Biochem. Mol. Biol. 37, 523–531. https://doi.org/10.1016/j.ibmb.2007.01.001.

Slater, A.F.G., Cerami, A., 1992. Inhibition by chloroquine of a novel haem polymerase enzyme activity in malaria trophozoites. Nature 355, 167–169. https://doi.org/10.1038/355167a0.

Slimen, I.B., Najar, T., Ghram, A., Dabbebi, H., Mrad, M.B., Abdrabbah, M., 2014. Reactive oxygen species, heat stress and oxidative-induced mitochondrial damage. A review. Int. J. Hypertherm. 30, 513–523. https://doi.org/10.3109/02656736.2014.971446.

Soni, A., Goyal, M., Prakash, K., Bhardwaj, J., Siddiqui, A.J., Puri, K., 2015. Cloning, expression and functional characterization of heme detoxification protein (HDP) from the rodent malaria parasite *Plasmodium vinckei*. Gene 566, 109–119. https://doi.org/10.1016/j.gene.2015.04.037.

Souza, A.V., Petretski, J.H., Demasi, M., Bechara, E.J., Oliveira, P.L., 1997. Urate protects a blood-sucking insect against hemin-induced oxidative stress. Free Radic. Biol. Med. 22, 209–214. https://doi.org/10.1016/s0891-5849(96)00293-6.

Sterkel, M., Oliveira, J.H.M, Bottino-Rojas, V., Paiva-Silva, G.O., Oliveira, P.L., 2017. The dose makes the poison: nutritional overload determines the life traits of blood-feeding arthropods. Trend. Parasitol. 33, 633–644. https://doi.org/10.1016/j.pt.2017.04.008.

Stiebler, R., Soares, J.B.R.C., Timm, B.L., Silva, J.R., Mury, F.B., Dansa-Petrestki, M., Oliveira, M.F., 2011. On the mechanisms involved in biological heme crystallization. J. Bioenerg. Biomembr. 43, 93–99. https://doi.org/10.1007/s10863-011-9335-x.

Tamura, K., Stecher, G., Kumar, S., 2021. MEGA11: molecular evolutionary genetics analysis version 11. Mol. Biol. Evol. https://doi.org/10.1093/molbev/msab120.

Terra, W.R., 1988. Physiology and biochemistry of insect digestion: an evolutionary perspective. Braz. J. Med. Biol. Res. 21 (4), 675–734.

Terra, W.R., Ferreira, C., 2012. Biochemistry and Molecular Biology of Digestion. Insect Molecular Biology and Biochemistry, [S.L.], 365-418. Academic Press. https://doi.org/10.1016/b978-0-12-384747-8.10011-x.

Vanlerberghe, G.C., 2013. Alternative oxidase: a mitochondrial respiratory pathway to maintain metabolic and signaling homeostasis during abiotic and biotic stress in plants. Int. J. Mol. Sci. 14, 6805–6847. https://doi.org/10.3390/ijms14046805.

Villiers, K.A., Egan, T.J., 2021. Heme detoxification in the malaria parasite: a target for antimalarial drug development. Acc. Chem. Res. 54, 2649–2659. https://doi.org/10.1021/acs.accounts.1c00154.

Walter-Nuno, A.B., Taracena, M.L., Mesquita, R.D., Oliveira, P.L., Paiva-Silva, G.O., 2018. Silencing of iron and heme-related genes revealed a paramount role of iron in the physiology of the hematophagous vector *Rhodnius prolixus*. Front. Genet. 9, 1–21. https://doi.org/10.3389/fgene.2018.00019.

Waterhouse, A., Bertoni, M., Bienert, S., Studer, G., Tauriello, G., Gumienny, R., Heer, F. T., de Beer, T.A.P., Rempfer, C., Bordoli, L., Lepore, R., Schwede, T., 2018. SWISS-MODEL: homology modelling of protein structures and complexes. Nucl. Acid. Res. 46, W296–W303. https://doi.org/10.1093/nar/gky427.

Winston, W.M., Molodowitch, C., Hunter, C.P., 2002. Systemic RNAi in *C. elegans* requires the putative transmembrane protein SID-1. Science 295, 2456–2459. https://doi.org/10.1126/science.1068836.

World Health Organization. Chagas Disease (American trypanosomiasis). 2022. Global distribution of cases of Chagas disease, based on official estimates, 2018. Avaialable on: https://cdn.who.int/media/docs/default-source/ntds/chagas-disease/chagas-2018-cases.pdf?sfvrsn=f4e94b3b_2.

Xu, D., Zhang, Y., 2011. Improving the physical realism and structural accuracy of protein models by a two-step atomic-level energy minimization. Biophys. J. 101, 2525–2534. https://doi.org/10.1016/j.bpj.2011.10.024.